Journal of Energy Resources Technology. Received August 28, 2019;
Accepted manuscript posted November 20, 2019. doi:10.1115/1.4045733

Surrogate Modeling for Capacity Planning of Charging Station Equipped with PV and Hydropneumatic Energy Storage

Yang Chen*
Environmental Sciences Division
Oak Ridge National Laboratory
Oak Ridge, U.S.

Fadwa Dababneh
Department of Manufacturing Engineering
Georgia Southern University
Statesboro, U.S.

Bei Zhang
GEIRI
Global Energy Interconnection
Research Institute, San Jose, U.S.

Saiid Kassaee
Department of Mechanical,
Aerospace, and Biomedical Engineering
University of Tennessee, Knoxville, U.S.

Brennan T. Smith
Environmental Sciences Division
Oak Ridge National Laboratory
Oak Ridge, U.S.

Xiaobing Liu, Ayyoub M. Momen
Energy and Transportation Science Division
Oak Ridge National Laboratory
Oak Ridge, U.S.

ABSTRACT

Due to promising potential for environmental sustainability, there has been a significant increase of electric vehicles (EVs) and plug-in hybrid electric vehicles (PHEV) in the market. To support this increasing demand for EVs and PHEVs, challenges related to capacity planning and investment costs of public charging infrastructure must be addressed. Hence, in this paper, a capacity planning problem for charging stations is developed and aims to balance current capital investment costs and future operational revenue. The charging station is assumed to be equipped with solar photovoltaic panel (PV) and an energy storage system which could be electric battery or recently invented hydro-pneumatic energy storage (GLIDES, Ground-Level Integrated Diverse Energy Storage) system. A co-optimization model that minimizes investment and operation cost is established to determine optimal solution while considering capacity planing and following operations. EV mobility is modeled as an Erlang-loss system. Meanwhile, stochastic programming is adopted to capture uncertainties from solar radiation and charging demand of EV fleet. To provide a more general and computationally efficient model, main configuration parameters are sampled in design space and then fixed in solving the co-optimization model. Sampled parameters include: EV charging slots number, PV area, capacity of energy storage system, and daily mean EV arrival number. Based on the sampled parameter combinations and its responses, black-box mappings are then constructed using surrogate models which could provide insights for charging station placement in different practical situations. The effectiveness of proposed surrogate modeling approach is demonstrated in numerical experiments. The results indicate better profit advantage of GLIDES over battery system with increased power capacity

*Corresponding Email: cheny2@ornl.gov.

1. INTRODUCTION

With benefits from environmental protection and energy security support, the transition to EVs is well underway with more than 1 million EVs on U.S. roads as of October 2018 [1]. In addition, customers are purchasing EVs in record numbers, and electric companies are working with stakeholders to move the EV infrastructure market forward [1]. The Edison Electric Institute and the Institute for Electric Innovation have developed a consensus forecast of EV sales projections from 2018 to 2030 and have estimated the associated charging infrastructure needs. It is projected that the number of EVs on the road will reach 18.7 million in 2030 and 9.6 million charge ports will be required, also, the next 1 million EVs will be manufactured in less than 3 years (i.e. by early 2021) [1].

To satisfy EVs charging demand, minimize initial investment and maximize profit in the long run for charging station, the sizing and capacity planning problem has gained significant interest in research and industry. For example, a completely green EV charging system is studied in [2] whose energy is generated exclusively by solar panels. To determine the optimal resource size (e.g., the number of solar panels and the energy-storage capacity), a search-based algorithm is devised to solve the formulated nonlinear integer programming problem more efficiently. A capacity determination model based on the queuing theory is developed to determine the amount of chargers needed in EV fast charging station, which is able to minimize the sum of waiting cost and charger cost [3]. A mixed-integer nonlinear optimization approach is present for optimal placing and sizing of the fast charging stations [4]. The model includes development cost, EV energy loss, electric grid loss as well as the location of electric substations and urban roads, and it is solved by genetic algorithm. It is stated that EVs are seen to have some negative impacts on micro-grid performance [5]. Inappropriate siting of charging stations could also have negative effects on city traffic network [6]. Optimization models are developed to obtain the optimal siting and sizing of charging stations with objectives of voltage variations network loss cost, charging cost, etc [5] [6]. The interactions between EV power demand and transportation networks is integrated [7]. Based on the assigned equilibrium traffic flow, a queuing model is then applied to determine the capacity of the charging station (number of charging devices) considering the constraints from both transportation and distribution networks. The possibility of charging battery EVs at workplace using solar energy is investigated [8] [9] and the feasibility of integrating a local storage to the EVPV charger to make it grid independent is evaluated. The results indicate that optimal storage size could reduce grid dependency by 25%. For different EV customer classes, they are distinguished by charging preferences, needs, and technologies. EV charging network equipped with different charging technologies is focused on [10] and two frameworks are proposed. One is appropriate for large networks where pricing dynamics is leveraged to control EV customer request rates and provide charging service with the best level of quality of service (QoS). The other one is more appropriate for smaller networks in which the objective is to compute the minimum amount of resources required to provide certain levels of QoS to each class. It also needs to be noted that, a new type of charging infrastructure is emerging based on the premise of battery swapping, and some latest studies have been put forward to optimize battery recharge schedule [11] [12]. Despite some advantages on shortening charging wait time, mitigating battery degradation, etc, some roadblocks still remain. For instance, standardization of EV Lithium Ion battery packs has not happened globally, reliability of leased/rented battery packs is not guaranteed. Also, public's adaption on this new mode is not fully investigated since the EV owners won't own the battery anymore, etc. Take Tesla for an example, in its pilot experiment with battery swapping technology stations in early 2013, only four or five EV owners out of 200 invitations responded to the test. [13].

In the aforementioned literature, a lot of research has been conducted to determine the location and optimal resource size in charging station. However, the very high capital cost [14] and degradation [15] [16] of battery storage pack has limited its deployment size and lifetime, thus reduced integration of more renewables and potential payback for charging station. With a recently invented and developed hydro-pneumatic energy storage technology (GLIDES) in Oak Ridge National Laboratory, in this study, the capacity planning problem of charging station is focused with special interest on the sizing of PV, storage power capacity (either battery storage or GLIDES system), and number of charging slots. The optimization objective considered here is the economic benefit for the charging station, including long term investment, maintenance cost and operation revenue. Our contribution could be summarized into three folds, 1) GLIDES is considered to be equipped in charging station and modeled in the operation, 2) for different possible configurations sampled from the design space, cost and profit of GLIDES are compared with the battery model, 3) several surrogate models are trained to predict best designs given different daily mean EV arrivals. With this clean and environment-friendly energy storage technology of GLIDES, the chemical and fire hazards are expected to be reduced effectively.

Based on the above objectives and considerations, the rest of the paper is organized as follows. In Section 2, first the GLIDES system is introduced, then capacity planning model is established for charging station, and this model is used to generate training data for reviewed surrogate models in Section 3. In Section 4, parameter setting and data generation are explained, followed by response surface of surrogate models for the design space. Finally, in Section 5, conclusions are drawn.

2. CAPACITY PLANNING OF CHARGING STATION

In this section, a capacity planning model is proposed, where solar PV system and energy storage system (two options: GLIDES and electric battery are used for comparison) are assumed to be equipped for charging station. Mobility of EV fleet is modeled as an Erlang-loss system. Therefore, the design space for the charging station is four-dimensional, [number of charging slots N, PV area S_{PV}, energy storage capacity S_{ES}, daily mean EV arrival number $\overline{A}$]. Each dimension has its own presumed value range. Please note that, the hourly EV arrival rate λ and the hourly EV charging rate μ will be sampled after the daily mean EV arrival number $\overline{A}$ is given.

The details on invented GLIDES storage are introduced next and then the capacity planning model is developed. For each sample (design combination) from the design space, this capacity planning model will be invoked to obtain the response (total system cost). This invoking process could be implemented in a parallel way.

2.1. GLIDES configuration

As descried in invention patent [17], a typical GLIDES system consists of a liquid storage reservoir, pre-pressurized pressure vessel(s), a pump/motor, and a hydraulic turbine/generator, see Figure 1. In the charging process, the electricity will drive the pump/motor to pump liquid from liquid storage reservoir to the pressure vessel(s) until certain pressure level (less than allowable maximum level in the vessel), in this process, the condensable gas (e.g. air, carbon dioxide, etc.) will be compressed and electricity is stored. To recover the stored energy, the now high-head water will be pushed by high pressure gas through the hydraulic turbine (e.g. Pelton turbine) which spins an electrical generator to dispatch electricity. More details on the GLIDES system and its thermal dynamics can be found in our previous studies [18] [19] [20].

As modular pump hydro storage, GLIDES system could be treated as the combination of Compressed Air Energy Storage (CAES) and conventional Pump Hydro Storage (PHS). The main difference between GLIDES and conventional PHS [21] is that it uses air pressure to create high water head instead of lifting the water body to a upper reservoir (usually in mountain top). The main difference between GLIDES and CAES [22] is that it uses general highly efficient hydraulic machinery (water pump/turbine) instead of gas compressor/turbine. This design has eliminated the geographical location limitation of conventional PHS (needs natural reservoirs) and improved the efficiency of compressed air storage. Comparing with electrochemical batteries, GLIDES system has neglectable degradation and maintenance effort, in addition, low grade heat could also be integrated to heat the top gas to further boost discharging efficiency. Storage technologies with the similar advantages could be found as Liquid Air Energy Storage in [23], Pumped Thermal Electricity Storage in [24]. In summary, GLIDES system has several main advantages: 1) it can be installed at ground level or below, basically anywhere that can structurally support the pressure vessels; 2) it has the ability to integrate a diverse range of low grade heat sources and use the waste heat to boost efficiency in the discharging process; 3) it is scalable by packing more pressure vessels which makes it possible to be allocated and utilized at the grid-scale or equipped for smart buildings for behind-meter applications (see modular version in Figure 2).

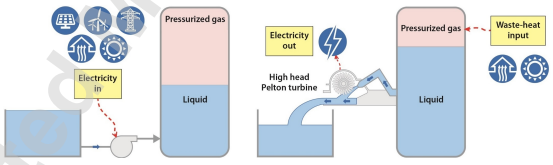

(a) Charging (b) Discharging

Fig. 1: Basic layout and components of GLIDES system

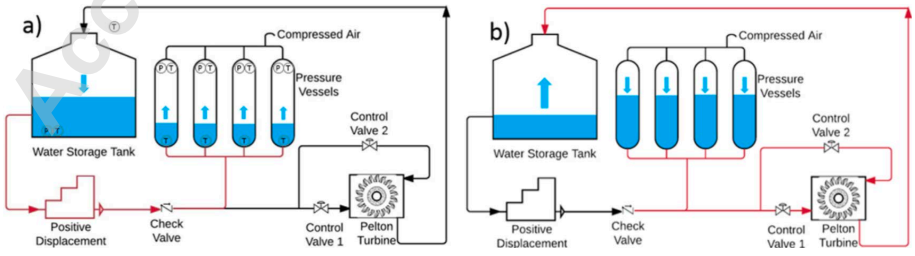

(a) (b)

Fig. 2: Modular GLIDES prototype schematic during charging a) and discharging b)

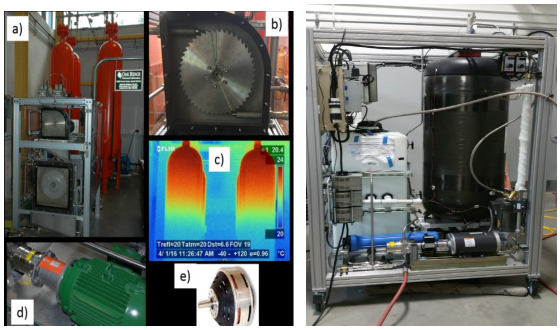

(a) first-generation (b) second-generation

Fig. 3: Prototypes of first (left figure, material: conventional steel) and second generation GLIDES (right figure, material: carbon fiber)

The first-generation GLIDES prototype (see Figure 3(a)) is sized at a nominal 3 kWh, energy is recovered using a Pelton turbine which can operate with two jets, delivering a peak 5.5 kW hydraulic power per jet. It is comprised of a 500-gallon water storage tank, four 500-liter carbon steel pressure vessels with maximum allowable working pressure of 160 bar, an 11 kW, 42 liter/min positive displacement pump/motor assembly, a custom-made, 2-jet Pelton turbine, and a 5 kW single phase 120 VAC 60 Hz electrical generator (not shown in Figure). The system was designed to operate with air as the gas and water as the liquid at pressures from minimum of 70 bar to maximum of 130 bar. Maximum pressure was limited to 130 bar in order to comply with laboratory safety regulations where the testing took place. In accounting for pump/motor, turbine and electric generator losses, the 91% indicated efficiency reduces to 66% round-trip efficiency for the first-generation GLIDES. For second generation GLIDES, 84% round-trip efficiency could be achieved. Please note that the round-trip efficiency greatly depends on different configuration and turbomachinery efficiencies [18] [19].

2.2. Mathematical Model

All the parameters and decision variables are listed in Table 1.

Table 1: Notation table for capacity planning model

Acronym	
BG, SG	Buying from, selling to power grid
PV, CS, EV	Solar panel, charging slots, electric vehicles
GS, BS, ES	GLIDES, battery, energy storage deployed (GS, BS)
PM, MO, TR, GT	Pump, motor, turbine, generator in GS
Design Variables	
S_{PV}, S_{ES}	Designed PV area, Energy storage capacity
$N_{CS}, \overline{A}$	Charging slot number, daily mean EV arrival number
Design Parameters	
U, M, L_p, r	Unit cost, Maint. cost, project lifetime, interest rate
N_{ES}	Battery cell number for BS, or vessel number for GS
Operation Parameters	
$\widetilde{R}, \gamma$	Stochastic electricity price, coef. of degradation cost
$\widetilde{Sol}, \eta$	Stochastic solar radiation level, efficiency
$\widetilde{\lambda}, \mu$	Stochastic EV arriving rate, charging rate
$\underline{PG}, \overline{PG}$	Min, max limit for power exchange
$\underline{\alpha}, \overline{\alpha}$	Coef. of lower and upper storage limits (BS & GS)
$\underline{\beta}, \overline{\beta}$	Coef. of dis-/charging power limits (BS & GS)
$\underline{V}, \overline{V}$	Min, max liquid volume in GS
$\underline{F}, \overline{F}$	Min, max liquid flow rate in GS
$\underline{PS}, \overline{PS}$	Min, max air pressure in GS
Operation Variables	
p, e	Electricity power, energy level
xc, xd	Binary status of charging, discharging of BS
xp, xg	Binary status of pumping/generating of GS

vc, vd	charging, discharging flow rate of GS
v, ps	liquid volume level, pressure level in GS

A. Objective Function

The objective C_{Obj} here is to minimize capacity planning cost and subsequent operational cost.

$$C_{Inv} = U_{PV} \cdot S_{PV} + U_{ES} \cdot S_{ES} + U_{CS} \cdot S_{CS} \tag{1}$$

$$C_{Mtn} = M_{PV} \cdot S_{PV} + M_{ES} \cdot S_{ES} + M_{CS} \cdot S_{CS} \tag{2}$$

$$C^s_{Opr,t} = \begin{bmatrix} \widetilde{R}^s_{BG,t} \cdot p^s_{BG,t} - \widetilde{R}^s_{SG,t} \cdot p^s_{SG,t} \\ -R^s_{EV,c,t} \cdot p^s_{EV,c,t} + \gamma_{ES} \cdot (p^s_{ES,c,t} + p^s_{ES,d,t}) \end{bmatrix} \tag{3}$$

$$C_{Obj} = \textstyle\sum_{s,t} \omega^s \cdot C^s_{Opr,t} - C_{Inv} \cdot \frac{r\cdot(1+r)^{Lp}}{(1+r)^{Lp}-1} - C_{Mtn} \tag{4}$$

C_{Inv}, C_{Mtn} denote the investment and maintenance costs, which are a function of three main design components of the charging station: solar panel area, energy storage capacity, charging slots. $C^s_{Opr,t}$ is the operation cost for each scenario s at time t, including revenue from selling electricity to power grid and EV fleets, payment for electricity bought from the power grid and EV fleets, and degradation cost from frequent charging/discharging of the energy storage system and EV fleets. ω^s is the scenario probability. Note that the investment cost C_{Inv} needs to be converted and allocated into the unit planning period based on the interest rate (see Eq.(4)), say 1 year.

B. Power Balance

The power balance between generation and demand is modeled in Eq.(5)-(7).

$$p^s_{PV,t} \le S_{PV} \cdot \widetilde{Sol}^s_t \cdot \eta_{PV} \tag{5}$$

$$\underline{PG} \le p^s_{GS,t} + p^s_{GB,t} \le \overline{PG} \tag{6}$$

$$p^s_{PV,t} + p^s_{GB,t} + N_{ES} \cdot p^s_{ES,d,t} + p^s_{EV,d,t} = p^s_{GS,t} + N_{ES} \cdot p^s_{ES,c,t} + p^s_{EV,c,t} \tag{7}$$

The PV power generation is modeled in Eq.(5) using an inequality constraint to allow the PV generation to be curtailed when necessary. The power exchange between the charging station and power grid is restricted by Eq.(6) to limit the impact on power grid. System-wide power generation and consumption is balanced in Eq.(7). N_{ES} can be used to represent either the battery cell number or pressure vessel number depending on which energy storage technology is chosen.

C. EV Battery Dynamics

To model the mobility of EV fleet, $M/M/n/n$ Queue (Erlang-loss system) is adopted [25] where EV arrivals are assumed to follow a Poisson process and their charging times are exponentially distributed. Aggregated EV charging behavior is modeled through Eq.(10)-Eq.(12).

$$Pr^s_{bl,t} = [(\widetilde{\lambda}^s_t/\mu)^{N_{CS}}/N_{CS}!] \cdot [\textstyle\sum_n^{N_{CS}} (\widetilde{\lambda}^s_t/\mu)^n/n!]^{-1} \tag{8}$$

$$\overline{M}^s_t = (\widetilde{\lambda}^s_t/\mu) \cdot [1 - Pr^s_{bl,t}] \tag{9}$$

$$e^s_{EV,t} = e^s_{EV,t-1} + (p^s_{EV,c,t} \cdot \eta_{EV} - p^s_{EV,d,t}/\eta_{EV}) \tag{10}$$

$$e^s_{EV,t=T} \ge E^s_{EV,0} + \overline{D}_{EV} \cdot \textstyle\sum_t^T \{\widetilde{\lambda}^s_t \cdot [1 - Pr^s_{bl,t}]\} \tag{11}$$

$$\left|e^s_{EV,t} - e^s_{EV,t-1}\right| \le (1 - \delta^s_{EV,t}) \cdot \overline{S}_{EV} \cdot \overline{M}^s_t \tag{12}$$

Accordingly, the probability that the charging station is full or blocked Pr_{bl} and the hourly mean number of charging customers $\overline{M}$ are calculated in Eq.(8) and Eq.(9). $\widetilde{\lambda}$, μ, N_{CS} are EV arriving rate (how many EV arrivals averagely in one hour), EV charging rate (how many EV are charged averagely in one hour for one charging slot), and total number of charging slots. $e^s_{EV,t}$ is stored energy level in EVs, $\overline{D}_{EV}$ is average energy demand of EVs, $\overline{S}_{EV}$ is average battery capacity of EVs. $\delta^s_{EV,t}$ is utilization factor of EV battery.

D. Energy Storage Dynamics

For the energy storage system equipped in the charging station, two options are considered and compared. One is battery storage system and the other one is GLIDES system. The two energy storage systems are modeled exclusively, however,

both share the same design variable for capacity S_{ES}. For the GLIDES, the power capacity S_{ES} are then used in Eq.(13)-(15) to calculate the size SV of the pressure vessel and max liquid volume $\overline{V}_{GS}$.

$$E_{st} = \frac{\overline{PS} \cdot (\overline{PS}/\underline{PS})^{-\frac{1}{m}} - \underline{PS}}{m-1} \tag{13}$$

$$SV = \frac{S_{ES} \cdot storagetime}{\eta_{RTE} \cdot E_{st}} \tag{14}$$

$$\overline{PS}/\underline{PS} = [(SV - \underline{V}_{GS})/(SV - \overline{V}_{GS})]^m \tag{15}$$

Eq.(13) is used to calculate the energy stored per unit of volume $joules/m^3$ in the compression/expansion process. This relationship will be used along with the desired power capacity S_{ES}, storage time and estimated round-trip-efficiency to calculate the required pressure vessel size SV using Eq.(14). The maximum liquid volume in the pressure vessel is obtained using Eq.(15). m is polytropic index.

(1) battery storage system (BS)

$$xc^s_{BS,t} + xd^s_{BS,t} \leq 1 \tag{16}$$

$$S_{ES} \cdot \underline{\alpha}_{BS} \leq e^s_{ES,t} \leq S_{ES} \cdot \overline{\alpha}_{BS} \tag{17}$$

$$e^s_{ES,t} = e^s_{ES,t-1} + (p^s_{ES,c,t} \cdot \eta_{BS} - p^s_{ES,d,t}/\eta_{BS}) \tag{18}$$

$$S_{ES} \cdot \underline{\beta}_{BS} \cdot xc^s_{BS,t} \leq p^s_{ES,c,t} \leq S_{ES} \cdot \overline{\beta}_{BS} \cdot xc^s_{BS,t} \tag{19}$$

$$S_{ES} \cdot \underline{\beta}_{BS} \cdot xd^s_{BS,t} \leq p^s_{ES,d,t} \leq S_{ES} \cdot \overline{\beta}_{BS} \cdot xd^s_{BS,t} \tag{20}$$

The charging/discharging behavior of the BS is modeled in Eq.(16)-Eq.(20). If BS is adopted to be deployed in charging station, then the capacity planning model becomes [Eq.(1)-Eq.(12), Eq.(16)-Eq.(20)].

(2) GLIDES storage system (GS)

$$xp^s_{GS,t} + xg^s_{GS,t} \leq 1 \tag{21}$$

$$\underline{V}_{GS} \cdot \underline{\alpha}_{GS} \leq v^s_{GS,t} \leq \overline{V}_{GS} \cdot \overline{\alpha}_{GS} \tag{22}$$

$$v^s_{GS,t} = v^s_{GS,t-1} + (vc^s_{GS,t} - vd^s_{GS,t}) \tag{23}$$

$$\overline{V}_{GS} \cdot \underline{\beta}_{GS} \cdot xp^s_{GS,t} \leq vc^s_{GS,t} \leq \overline{V}_{GS} \cdot \overline{\beta}_{GS} \cdot xp^s_{GS,t} \tag{24}$$

$$\overline{V}_{GS} \cdot \underline{\beta}_{GS} \cdot xg^s_{GS,t} \leq vd^s_{GS,t} \leq \overline{V}_{GS} \cdot \overline{\beta}_{GS} \cdot xg^s_{GS,t} \tag{25}$$

$$ps^s_{GS,t}/PS_0 = [\overline{V}_{GS} - V_0]/[\overline{V}_{GS} - v^s_{GS,t}]^m \tag{26}$$

$$p^s_{ES,c,t} \cdot \eta_{PM} \cdot \eta_{MO} \leq vc^s_{GS,t} \cdot ps^s_{GS,t} \tag{27}$$

$$p^s_{ES,d,t}/(\eta_{TR} \cdot \eta_{GT}) \leq vd^s_{GS,t} \cdot ps^s_{GS,t} \tag{28}$$

Instead of the BS, if the GLIDES system is chosen, then Eq.(21)-Eq.(28) will be included in the model, and the capacity planning model becomes [Eq.(1)-Eq.(15), Eq.(21)-Eq.(28)].

In the charging/discharging process, the liquid volume v in the pressure vessel and the liquid speed vc, vd are restricted by $[\underline{V}, \overline{V}]$ and $[\underline{F}, \overline{F}]$. Eq.(26) comes from polytropic gas compression/expansion process between a minimum and maximum pressure Pascal. This models the relationship between the gas pressure ps and liquid volume v in the vessel where PS_0 and V_0 are the initial pressure and liquid volume. Moreover, the power exponent m is the polytropic index, set to be 1.2 based on the experimental data available from first lab-scale proof-of-concept GLIDES prototype in ORNL. In the charging/discharging process, the electricity power could be calculated using the fluid power equations in Eq.(27)-Eq.(28).

3. SURROGATE MODEL FOR CO-OPTIMIZATION

A surrogate model (or meta-model/ response surface) involves model fitting or function approximation of the sampled data from the design variables and responses based on the detailed analytical model [26]. Of particular interest, one regression based and two interpolation based meta-models are considered. Since our responses will be simulated from the mathematical model proposed in previous section,a noise-free fitting process is appropriate.

(a) Polynomial regression model (PR)

Polynomial regression is derived as the general version of linear regression, which has been extensively applied in data learning domains. As a parametric technique, some functional relationship (e.g. the polynomial order) will be presumed and chosen for the design variables and the responses [27].

$$\hat{f}(\mathbf{x}) = \sum_{i=1}^{n_b} w_i \psi^i \tag{29}$$

where, $\hat{f}$ is function approximation for variables vector $\mathbf{x}$, ψ is the basis function, and n_b is total number of basis functions, For instance, with polynomial order 2, $\psi \in \{1, x_1, x_2, x_1x_2, x_1^2, x_2^2\}$. w_i is the unknown coefficient which directly reflect the significance of different design variables, it is usually obtained by least squares method.

(b) Radial basis function model (RBF)

The RBF model gives predictions based on the weighted combination of the distances between the prediction site $\mathbf{x}$ and the centres $\mathbf{c}^{(i)}$ of the basis functions [28]. RBF is a single-layer neural network with radial coordinate neurons, and demonstrates very good performance on highly nonlinear mapping relationships in a number of literature. It has the fixed form in Eq.(30).

$$\hat{f}(\mathbf{x}) = \mathbf{w}^T \boldsymbol{\psi} = \sum_{i=1}^{n_c} w_i \psi(||\mathbf{x} - \mathbf{c}^{(i)}||) \tag{30}$$

where, $\mathbf{c}^i$ denotes the ith of the n_c basis function centres and $\boldsymbol{\psi}$ is the n_c-vector containing the values of the basis functions ψ themselves. w_i is the unknown interpolation coefficient which could be easily determined using interpolation conditions. Several popular basis functions for RBF are fixed functions: cubic $\psi(r) = r^3$, thin plate spline $\psi(r) = r^2 \ln r$, more freedom with parametric function: Gaussian $\psi(r) = e^{-r^2/(2\sigma^2)}$, multiquadric $\psi(r) = (r^2 + \sigma^2)^{1/2}$, etc, σ has to be tuned.

(c) Kriging model (Kriging)

Kriging (also know as Gaussian process regression) is an interpolation method [29], assuming that the deviations from regression model $F(\mathbf{x})\boldsymbol{\beta}$, even though the responses may in fact be deterministic, may resemble a sample path of a (suitably chosen) stochastic process Z with zero mean and stationary covariance. The correlations are given by kriging basis function Eq.(33) which depends on the absolute distance between the sample points $|x_j^i - x_j^l|$ and the parameters p_j and θ_j.

$$\hat{f}(\mathbf{x}) = F(\mathbf{x})\boldsymbol{\beta} + Z(\mathbf{x}) \tag{31}$$

$$F(\mathbf{x}) = [f(\mathbf{x}^{(1)}), \ldots, f(\mathbf{x}^{(n)})] \tag{32}$$

$$Cov[Z(\mathbf{x}^i), Z(\mathbf{x}^l)] = \sigma^2 \boldsymbol{\psi} \tag{33}$$

$$\psi^{(i)} = exp(-\sum_{j=1}^{k} \theta_j |x_j^{(i)} - x_j)|^{p_j}) \tag{34}$$

where $\boldsymbol{\beta}$ is the weight vector, k is the index for design variables, i and l are indices of sample points n. Compared to the Gaussian radial basis function with $1/\sigma^2$ in RBF ($\psi(r) = e^{-r^2/(2\sigma^2)}$), the kriging basis function has a vector $\boldsymbol{\theta}$ allowing the width of the basis function to vary from variable to variable, which indicates the importance of this variable due to its large influence. The exponent $\boldsymbol{p}$ allows the degree of each dimension of design variables x to vary (typically $p_j \in [1, 2]$). When $\boldsymbol{\theta}$ is constant and $\boldsymbol{p} = 2$, kriging basis will be exactly the same as Gaussian radial basis function $\psi(r) = e^{-r^2/(2\sigma^2)}$. Kriging gives best linear unbiased predication, but the computation of parameter $\boldsymbol{\theta}$ and $\boldsymbol{p}$ in correlation function could be time consuming using maximum likelihood estimation.

General steps of surrogate modeling process [30] follows the flowchart in Figure 4. In step 1, Latin Hypercube Sampling is adopted for design space sampling; the proposed optimization model is used to generate the training data set in step 2; for the chosen surrogate models in step 3, a cross-validation approach is used to evaluate the model performance in step 4; in the last step, if the mean squared error is within the tolerance limit, then the process terminates, otherwise, new designs will be added to previous samples (please note that the latin property has to be maintained).

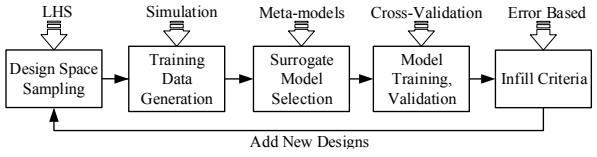

Fig. 4: Overall surrogate modeling process

4. NUMERICAL EXPERIMENTS

4.1. Scenario Generation and Parameters

For the listed four design variables in Table 1, they are sampled in a 4-dimensional space using space filling technic (Latin Hypercube Sampling). Their value range is assumed as: $S_{PV} \in [200, 1000]$ (m^2), $S_{ES} \in [100, 800]$ (kW), $N_{CS} \in [5, 25]$, $\overline{A} \in [0, 150]$. Totally 2000 design combinations (design points) are sampled from the design space initially.

In proposed capacity planning model, a typical summer day (middle of July) and winter day (middle of January) are chosen to simulate the operation, and the summed objective value of these two days are multiplied by 366/2 to estimate a whole year's operational objective. Three stochastic parameters are considered in the operation, electricity purchasing price $\widetilde{R}_{BG}$ (electricity selling price $\widetilde{R}_{SG}$ is assumed to be the same), solar radiation $\widetilde{Sol}$ [31] [32], EV arriving rate $\widetilde{\lambda}$ [33]. To simulate the randomness, these three parameters are sampled uniformly with fluctuation range $\pm 30\%$ based on their base level. Initially 100 scenarios are sampled. To reduce the computational burden and capture main stochastic information, simultaneous backward method [34] is implemented to trim down the deteriorated scenarios. Initial 100 scenarios are reduced to 5 final scenarios. The final scenarios are plotted for these three parameters, Figure 5(a), 5(b), 5(c). EV charging price [35] is also given in Figure 5(d). Please note that, the generated hourly EV arriving rate will be adjusted randomly to ensure total EV arrival number equals the specific designed daily mean EV arrival number $\overline{A}$.

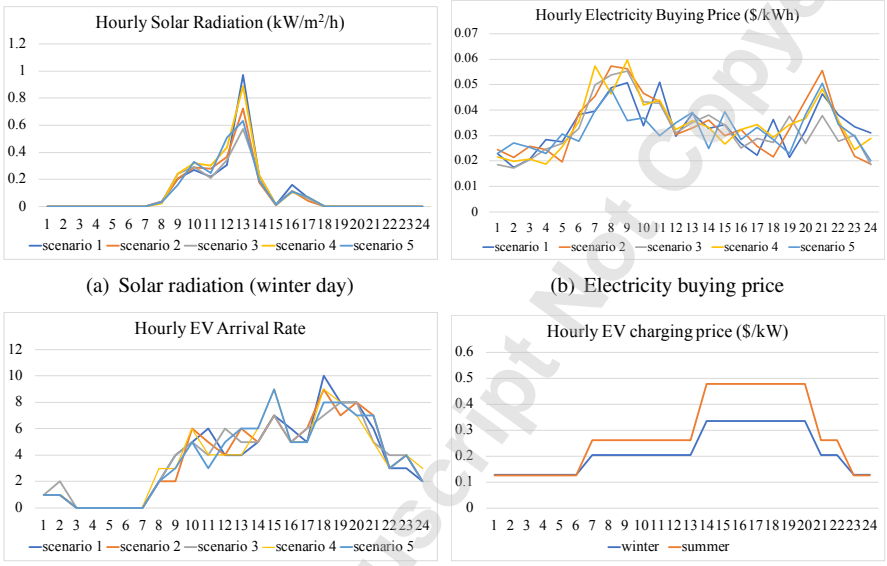

(a) Solar radiation (winter day)

(b) Electricity buying price

(c) Hourly EV arrivals ($\overline{A} = 90$)

(d) EV charging price

Fig. 5: Plots for $\widetilde{Sol}$, $\widetilde{R}_{BG}$, $\widetilde{\lambda}$, $R_{EV,c}$

Table 2: Parameters for one battery cell in battery storage

$[U_{BS}, \gamma_{BS}]$($/kW)	M_{BS}($/kW/yr)	$\underline{\alpha}_{BS}, \overline{\alpha}_{BS}$	$\underline{\beta}_{BS}, \overline{\beta}_{BS}$	η_{BS}
[1533, 0.008]	20	0.05, 1	0.1, 0.25	0.95

Table 3: Parameters for one pressure vessel in GLIDES system

$SV(m^3)$	$[\underline{PS}, \overline{PS}]$ (kpa)	$[\underline{V}, \overline{V}]$ (m^3)	V_0, P_0	η_{PM}, η_{MO}
92.331	[7000, 13000]	[0, 37.211]	18.605, 9170.095	0.9, 0.9
η_{TR}, η_{GT}	$\underline{\alpha}_{GS}, \overline{\alpha}_{GS}$	$\underline{\beta}_{GS}, \overline{\beta}_{GS}$	$[U_{GS}, \gamma_{GS}]$($/kW)	M_{GS}($/kW/yr)
0.9, 0.9	0, 1	0.1, 0.25	[700, 0]	0

For the purpose of comparing battery storage and GLIDES system, we assume one battery cell and one pressure vessel for GLIDES has same power capacity 20 kW and 4 hours discharging duration (fixed duration length for all samples). Then the final cell number and vessel number can be determined once the designed power capacity is sampled. The other parameters of battery and GLIDES are also listed in Table 2 and Table 3 equivalently. Unit cost of battery (medium duration

0.5-2 hours) is adopted from market report [14], maintenance cost is adopted from reference [36]. And degradation cost of battery could be estimated based on reference [16], $\gamma_{BS} = \frac{U_{BS}}{24 \cdot 365 \cdot 20}$, assume the lifetime of battery is 20 years. Unit cost U_{GS} of GLIDES depends greatly on the material that pressure vessel is made of, e.g. high-pressure pipe segments, carbon fiber, steel, etc. The cost details and reduction opportunities of GLIDES system could refer to [37] [38]. Maintenance cost M_{GS} for GLIDES is assumed to be zero here, but it needs to be noted that it will raise some non-neglectable cost if a more complex-higher efficiency system is used. All components efficiency of GLIDES system are set to be 0.9, e.g, efficiencies of pump, motor, turbine and generator. Other parameters are set as: $\underline{PG}, \overline{PG} = [0, 1000]$ (kW), EV charging rate $\mu = 1$, project lifetime $L_p = 50$ year (yr), interest rate $r = 0.05$, unit cost $U_{CS} = 3600$\$, $U_{PV} = 508$\$, maintenance cost $M_{CS} = 80$\$/yr, $M_{PV} = 10$\$/m^2/yr. PV efficiency $\eta_{PV} = 0.75$, average EV battery capacity $\overline{S}_{EV} = 100$kW, average EV demand $\overline{D}_{EV} = 40$kW, utilization factor of EV battery $\delta_{EV} = 0$.

4.2. One Day's Operation of GLIDES

To better illustrate the operation of GLIDES system in charging station, one summer day is chosen to demonstrate volume-pressure relationship in charging/discharging operation of GLIDES. The design sample (point) is given as $S_{PV} = 897$m^2, $S_{ES} = 385$kW, $N_{CS} = 14$, $\overline{A} = 90$. To weak the potential impact from previous day, the final level in the end hour of each day is demanded to be the same as initial level V_0 in Table 3. The liquid volume and gas pressure level in the pressure vessel is shown in Figure 6.

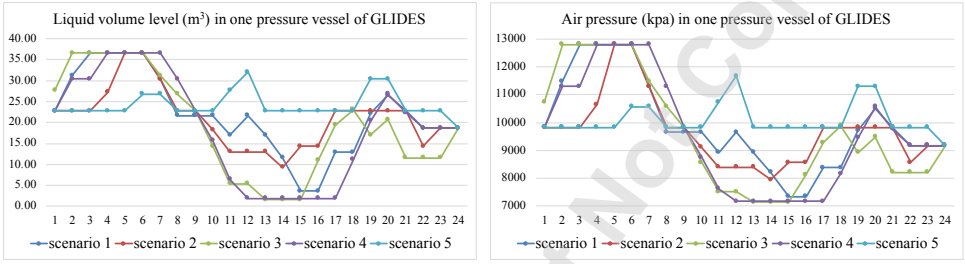

(a) Liquid volume level (b) Air pressure level

Fig. 6: Volume and pressure level in one pressure vessel of GLIDES

Following the electricity price pattern in Figure 5(b), generally, the liquid is pumped into storage vessel during non-peak hours (about hour 1-3 and hour 17-20), and the gas is squeezed above with pressure increasing. In peak hour periods, the pressure vessel discharges the liquid flow through hydraulic turbine which drives an electrical generator to generating power. Please note that, this operation curve is not only resulted by electricity price alone but also the solar radiation level, total charging demand from EVs, etc.

4.3. Response Surface of Surrogate Models

In this subsection, the surrogate models (PR, RBF, Kriging) are trained and constructed based on all the design samples. The annual net profit (C_{Obj} in Eq.(4)) is aimed and chosen as the response or dependent variable in the training process, and the four design variables, S_{PV}, S_{ES}, N_{CS}, $\overline{A}$ are the independent variables.

As mentioned, the operational revenue from summer and winter day are summed together and times 366/2 to estimate one year's operational revenue. For the comparison purpose, the converted annual investment cost, annual maintenance cost and annual operational revenue are shown in Figure 7 for the first 100 design samples for both battery storage and GLIDES, the power capacity of the first 100 samples covers from 100 kW to 790 kW. Note that the 100 samples on x-axis are in ascending order based on energy storage capacity S_{ES} only, the other three design variables are not in any order. Under current data settings, for each sampling configuration, GLIDES system has great advantage on investment and maintenance cost in Figure 7(a) and Figure 7(b). When the power capacity is lower, for example the sample point 2 and sample 15 in Figure 7(e), battery system could have a slightly better net profit depends on other design variables. After the sample 16 on x-axis (around 200 kW), even though the operational revenue with GLIDES system is lower than the design with battery system, net profit for the design with GLIDES system is still higher than the design with battery system and increasing. This result indicates that, due to high round trip efficiency, the design with battery system has a better operational revenue while net profit prefers GLIDES system when all investment are included, and the advantage of GLIDES increases along with needed capacity in Figure 7(e). Please note that, revenue and net profit could be negative if the designed power capacity is too large and mean daily EV arrival number through the year is not big enough to cover total cost.

Journal of Energy Resources Technology. Received August 28, 2019;
Accepted manuscript posted November 20, 2019. doi:10.1115/1.4045733

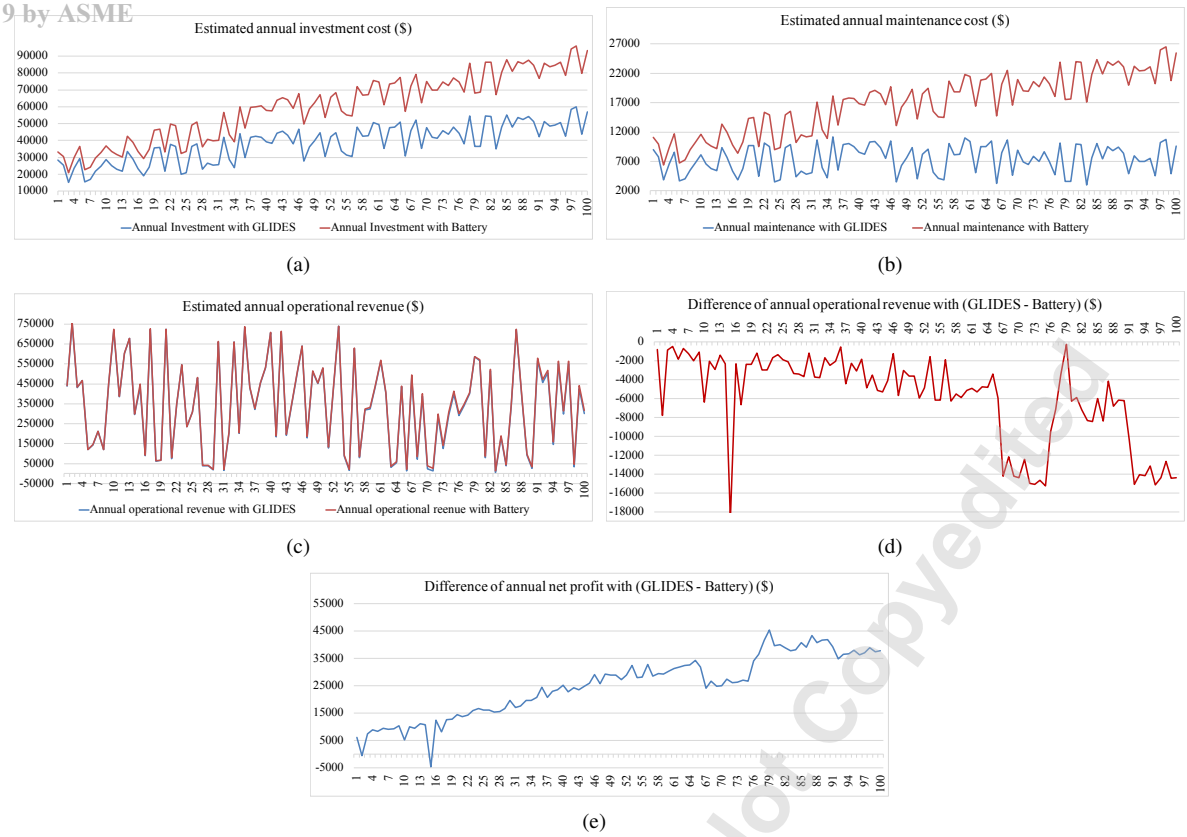

Fig. 7: Annual cost comparison for battery and GLIDES

Table 4: NRMSE metrics for trained surrogate models

–	PR	RBF	Kriging	Mix-KgPc	Mix-RcPc
Battery	0.0343	0.0430	0.0068	0.0091	0.0349
GLIDES	0.0356	0.0436	0.0112	0.0142	0.0359

Based on all samples, totally five surrogate model are developed: PR with cubic, RBF model with cubic radial basis function, Kriging model with Gaussian correlation function and second order regression polynomial model, also two mixed model Mix-KgPc (ensambled Kriging and PR model) and Mix-RcPc (ensambled RBF and PR model). Each model is validated using a cross-validation approach, 10-fold cross validation is applied with splitting 90% samples as training subset and 10% as validation subset to prevent over-fitting. An accuracy measure, normalized root mean square error (NRMSE), is used to evaluate the performance of each surrogate models, see Table 4. It is observed that interpolation Kriging model works best for both battery storage and GLIDES system, and is chosen for prediction purpose.

When daily mean EV arrival number could be estimated in a certain area, sliced response cubes in the remaining 3D design space (PV area, Storage capacity, Number of charging slots) could be generated. Take GLIDES system as an example, Kriging model is adopted to predict annual net profit in the design space, see Figure 8(a)-8(b). When daily mean EV arrival number is very small, for example, $\overline{A} = 5$ in Figure 8(a), the best configuration is given at 724 m^2 PV, 166 kW power capacity for GLIDES and 20 charging slots, with predicted annual net profit \$5.32 $\times$ 10^4. It could result in negative incoming if initial investment is too high. With increased EV arrivals, $\overline{A} = 55$, the most potential profit area moves towards a larger storage capacity, the best configuration is at [1000 m^2, 222 kW, 24] with estimated annual net profit \$2.54 $\times$ 10^5.

Although trained surrogate models are much more efficiency in depicting the solution space than conventional optimization models, it needs to be aware of some common limitations in meta-model techniques. First of all, a uniform level of model accuracy throughout the design space requires a uniform spread of sample points, the adopted sampling techniques and sample numbers will greatly determine prediction accuracy. Secondly, the key limitation is so-called “curse of dimensionality”, if the problem being dealt with has many dimensions, the number of points needed to give reasonably uniform coverage rises exponentially.

Journal of Energy Resources Technology. Received August 28, 2019;
Accepted manuscript posted November 20, 2019. doi:10.1115/1.4045733

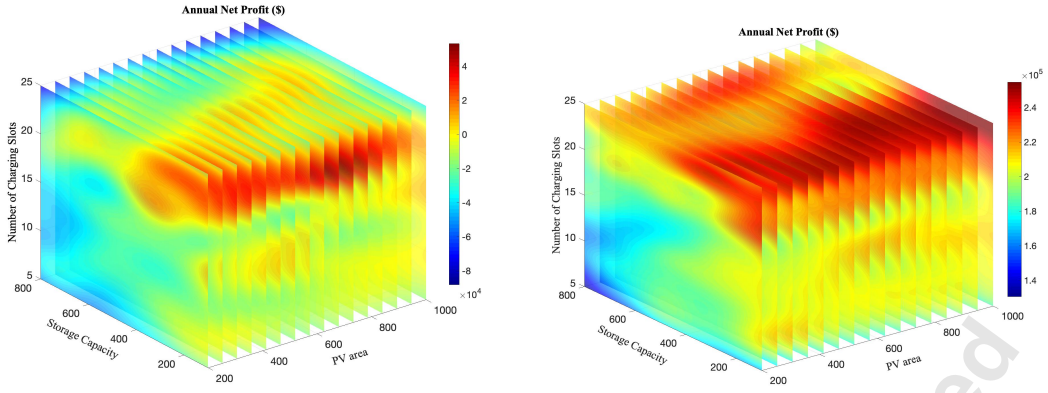

(a) (b)

Fig. 8: Sliced response cube for annual net profit ($\overline{A} = 5$) and ($\overline{A} = 55$)

5. CONCLUSION

In this research, sizing optimization for charging station is studied with the objective of maximizing possible annual net profit composed of initial investment, maintenance cost and subsequent operation revenue. Capacity planning model is proposed first with the operation of battery storage or GLIDES system. Annual cost comparison has shown GLIDES system is more cost beneficial in terms of lower lifetime capital cost, maintenance cost and thus higher net profit. Although battery system could have a better profit due to high efficiency when power capacity is low, it is safe to conclude that GLIDES system will performs better than battery system in final profit when needed power capacity increases (in the studied case here, after 200 kW). Considering the range of arrived EV in different area, surrogate modeling is adopted to build more general data-driven decision models. With trained interpolation Kriging model, the meshgrid response surface in the whole design space are plotted, which gives annual profit prediction for different design configurations. For future study, other behind-meter applications of GLIDES (e.g. in smart buildings) will be focused and the ability of GLIDES in integrating possible low-grade waste heat sources will be explored.

References

[1] Cooper, A., and Schefter, K., 2018. Report Electric Vehicle Sales Forecast and the Charging Infrastructure Required Through 2030. Tech. Rep. November, Edison Electric Institute & Institute of Electric Innovation.
[2] Ugirumurera, J., and Haas, Z., 2017. "Optimal Sizing of a Completely Green Charging System for Electric Vehicles". *IEEE Transactions on Transportation Electrification,* **3**(3), pp. 1–1.
[3] Dong, X., Mu, Y., Jia, H., Wu, J., and Yu, X., 2016. "Planning of Fast EV Charging Stations on a Round Freeway". *IEEE Transactions on Sustainable Energy,* **7**(4), pp. 1452–1461.
[4] Sadeghi-Barzani, P., Rajabi-Ghahnavieh, A., and Kazemi-Karegar, H., 2014. "Optimal fast charging station placing and sizing". *Applied Energy,* **125**, pp. 289–299.
[5] Moradi, M. H., Abedini, M., Tousi, S. M., and Hosseinian, S. M., 2015. "Optimal siting and sizing of renewable energy sources and charging stations simultaneously based on Differential Evolution algorithm". *International Journal of Electrical Power and Energy Systems,* **73**, pp. 1015–1024.
[6] Liu, Z., Wen, F., and Ledwich, G., 2013. "Optimal planning of electric-vehicle charging stations in distribution systems". *IEEE Transactions on Power Delivery,* **28**(1), pp. 102–110.
[7] Xiang, Y., Liu, J., Li, R., Li, F., Gu, C., and Tang, S., 2016. "Economic planning of electric vehicle charging stations considering traffic constraints and load profile templates". *Applied Energy,* **178**, pp. 647–659.
[8] Chandra Mouli, G. R., Bauer, P., and Zeman, M., 2016. "System design for a solar powered electric vehicle charging station for workplaces". *Applied Energy,* **168**(2016), pp. 434–443.
[9] Kuang, Y., Chen, Y., Hu, M., and Yang, D., 2017. "Influence analysis of driver behavior and building category on economic performance of electric vehicle to grid and building integration". *Applied Energy,* **207**, pp. 427 – 437.
[10] Bayram, I. S., Tajer, A., Abdallah, M., and Qaraqe, K., 2015. "Capacity Planning Frameworks for Electric Vehicle Charging Stations With Multiclass Customers". *IEEE Transactions on Smart Grid,* **6**(4), pp. 1934–1943.
[11] Schneider, F., Thonemann, U. W., and Klabjan, D., 2018. "Optimization of Battery Charging and Purchasing at Electric Vehicle Battery Swap Stations". *Transportation Science,* **52**(5), pp. 1211–1234.
[12] Sun, B., Tan, X., and Tsang, D. H. K., 2018. "Optimal charging operation of battery swapping and charging stations

with qos guarantee". *IEEE Transactions on Smart Grid,* **9**(5), Sep., pp. 4689–4701.
[13] Diwan, P., 2018. Is Battery Swapping a Viable Option for Public Transportation EVs?, https://medium.com/@pdiwan/is-battery-swapping-a-viable-option-for-public-transportation-evs-adb4ced74ff2.
[14] Energy Information Administration, U., 2018. U.S. Battery Storage Market Trends.
[15] Xie, L., Gu, Y., Eskandari, A., and Ehsani, M., 2012. "Fast mpc-based coordination of wind power and battery energy storage systems". *Journal of Energy Engineering,* **138**(2), pp. 43–53.
[16] Bordin, C., Anuta, H. O., Crossland, A., Gutierrez, I. L., Dent, C. J., and Vigo, D., 2017. "A linear programming approach for battery degradation analysis and optimization in offgrid power systems with solar energy integration". *Renewable Energy,* **101**, pp. 417–430.
[17] Momen, A. M., Kyle, J., Abdelaziz, O. A., Vineyard, E. A., Abu-heiba, A., and Odukomaiya, A. O., 2017. "Near isothermal combined compressed gas/pumped-hydro electricity storage with waste heat recovery capabilities". *Current Assignee: UT-Battelle LLC*, p. Patent No. US 2017/0082123 A1.
[18] Odukomaiya, A., Abu-Heiba, A., Gluesenkamp, K. R., Abdelaziz, O., Jackson, R. K., Daniel, C., Graham, S., and Momen, A. M., 2016. "Thermal analysis of near-isothermal compressed gas energy storage system". *Applied Energy,* **179**, pp. 948–960.
[19] Odukomaiya, A., Abu-Heiba, A., Graham, S., and Momen, A. M., 2018. "Experimental and analytical evaluation of a hydro-pneumatic compressed-air Ground-Level Integrated Diverse Energy Storage (GLIDES) system". *Applied Energy,* **221**(April), pp. 75–85.
[20] Chen, Y., Odukomaiya, A., Kassaee, S., OConnor, P., Momen, A. M., Liu, X., and Smith, B. T., 2019. "Preliminary analysis of market potential for a hydropneumatic ground-level integrated diverse energy storage system". *Applied Energy,* **242**, pp. 1237 – 1247.
[21] Prez-Daz, J. I., Chazarra, M., Garca-Gonzlez, J., Cavazzini, G., and Stoppato, A., 2015. "Trends and challenges in the operation of pumped-storage hydropower plants". *Renewable and Sustainable Energy Reviews,* **44**, pp. 767 – 784.
[22] Mazloum, Y., Sayah, H., and Nemer, M., 2016. "Static and Dynamic Modeling Comparison of an Adiabatic Compressed Air Energy Storage System". *Journal of Energy Resources Technology,* **138**(6), 05.
[23] Sciacovelli, A., Smith, D., Navarro, M. E., Vecchi, A., Peng, X., Li, Y., Radcliffe, J., and Ding, Y., 2017. "Performance Analysis and Detailed Experimental Results of the First Liquid Air Energy Storage Plant in the World". *Journal of Energy Resources Technology,* **140**(2), 11.
[24] McTigue, J. D., White, A. J., and Markides, C. N., 2015. "Parametric studies and optimisation of pumped thermal electricity storage". *Applied Energy,* **137**, pp. 800 – 811.
[25] Zhang, B., Yan, Q., and Kezunovic, M., 2017. "Placement of ev charging stations integrated with pv generation and battery storage". In 2017 Twelfth International Conference on Ecological Vehicles and Renewable Energies, pp. 1–7.
[26] Forrester, A. I. J., Sobester, A., and Keane, A. J., 2008. "Engineering design via surrogate modelling - a practical guide". In WILEY.
[27] Gano, S., Kim, H., and Brown, D., 2012. "Comparison of three surrogate modeling techniques: Datascape, kriging, and second order regression". In 11th AIAA/ISSMO Multidisciplinary Analysis and Optimization Conference.
[28] Bouhlel, M. A., Hwang, J. T., Bartoli, N., Lafage, R., Morlier, J., and Martins, J. R., 2019. "A python surrogate modeling framework with derivatives". *Advances in Engineering Software*, p. 102662.
[29] Nielsen, H. B., Lophaven, S. N., and Søndergaard, J., 2002. DACE - a matlab kriging toolbox.
[30] Chen, Y., Hu, M., and Zhou, Z., 2017. "A Data-Driven Analytical Approach to Enable Optimal Emerging Technologies Integration in the Co-Optimized Electricity and Ancillary Service Markets". *Energy,* **122**, pp. 613–626.
[31] Chen, Y., and Hu, M., 2016. "Balancing collective and individual interests in transactive energy management of interconnected micro-grid clusters". *Energy,* **109**, pp. 1075–1085.
[32] National Renewable Energy Laboratory, 2017. National Solar Radiation Data Base.
[33] Kim, J.-H., and Kim, C.-H., 2016. "Demand power with EV charging schemes considering actual data". *Journal of International Council on Electrical Engineering,* **6**(1), pp. 235–241.
[34] Gröwe-Kuska, N., Heitsch, H., and Römisch, W., 2003. "Scenario reduction and scenario tree construction for power management problems". *2003 IEEE Bologna PowerTech - Conference Proceedings,* **3**, pp. 152–158.
[35] PG&E, 2018. Electric vehicle (ev) rate plans, https://www.pge.com/en_us/residential/rate-plans/rate-plan-options/electric-vehicle-base-plan/electric-vehicle-base-plan.page?wt.mc_id=vanity_pevrates.
[36] DiOrio, N., Dobos, A., and Janzou, S., 2015. "Economic Analysis Case Studies of Battery Energy Storage with SAM". *Technical Report*(November).
[37] Kassaee, S., Abu-Heiba, A., Ally, M. R., Mench, M. M., Liu, X., Odukomaiya, A., Chen, Y., King, T. J., Smith, B. T., and Momen, A. M., 2019. "Part 1- techno-economic analysis of a grid scale ground-level integrated diverse energy storage (glides) technology". *Journal of Energy Storage,* **25**, p. 100792.
[38] Kassaee, S., Odukomaiya, A., Abu-Heiba, A., Liu, X., Mench, M. M., OConnor, P., and M. Momen, A., 2018. "Ground Level Integrated Diverse Energy Storage (GLIDES) Cost Analysis". In ASME International Mechanical Engineering Congress and Exposition, p. V06BT08A059.

List of Figures

List of Tables